Penning Trap Simulation

Sophus Gullbekk, Erlend Kristensen, Tov Tyvold, Jonathan Larsen
(Dated: July 28, 2022)

The aim of this report is to study an idealized version of a device called *Penning trap*. It is used by scientists all over the world to investigate charged particles by trapping them long enough to gather data. We simulate singly charged Ca^+ ions and explore how the ions interact with each other inside the trap. In addition, we will analyse two different numerical methods and figure out which one is best suited to perform the simulations.

I. INTRODUCTION

Utilizing a static configuration of electric and magnetic fields, the Penning trap can be used to measure properties through precise experiments. Trapping the various particles in all three dimensions using a quadruple electrostatic field. [1]

Unsurprisingly, it was a man called *F. M. Penning* who first described the fundamental idea that made the Penning trap possible. He proposed that you could improve the operation of a vacuum gauge by adding a magnetic field. This would force the electrons along a radial path inside the gauge.[2] This advantage caught the interest of *Hans Georg Dehmlet*. In 1973 he managed to observe, for the first time, a single trapped electron. Dehmlet received a *Nobel Prize in Physics* for his work in 1989,

> The g-factor anomaly has now been determined by Dehmelt and his co-workers with an accuracy of a few parts in a billion, and this, together with corresponding theoretical calculations, constitutes one of the most critical tests we have of QED. [3]

In modern times, the Penning trap technique has been further developed to create, store and cool antihydrogen. Being able to extract and use precise data from the experiment gives us the ability to further our understandings about matter and antimatter. The creativity surrounding Penning trap-physics are to this day still popular as trapping techniques are continuously a tool for progressing science. [4]

When introducing more than a single particle inside the trap, the equations of motions become non-linear. This makes it hard, if not impossible, to solve the equations analytically. Therefore we will solve them using numerical methods. In this report we analyze both the Euler-Cromer method and the Runge-Kutta 4 method. They enable the simulation of many particles inside the trap.

In section II we derive the physics and the functions that are crucial for our trap to work. This leads us to section III where we will demonstrate and study our results. The section will also consist of our own interpretation of the results. Lastly, in section IV we will put our findings together and make a statement regarding what we wanted to know and what the future might hold.

II. METHODS

A. The Physics Scenario

The Penning trap uses magnetic and electric fields to confine the particles. In our idealized Penning trap the electric field is defined by $\mathbf{E} = -\nabla\mathbf{V}$, where

$$V(x, y, z) = \frac{V_0}{2d^2}(2z^2 - x^2 - y^2). \tag{1}$$

Here V_0 is the voltage between **a** and **b** in figure 1 and d is the *characteristic dimension* which represents the size of the region between the electrodes where the particles are confined. The electric field make the particles stable in the z-direction, but they are still unstable in the xy-plane. Therefore we introduce a homogeneous magnetic field $\mathbf{B}$ to stop particles from escaping in the xy-plane. The homogenious magnetic field is given by $\mathbf{B} = B_0\hat{e}_z$, where B_0 is the field strength ($B_0 > 0$). This will accelerate the particles towards the centre of the trap, making them rotate around the centre of the trap. Together these fields confine the particles to a region inside the trap. See figure 1 for the schematics of the trap.

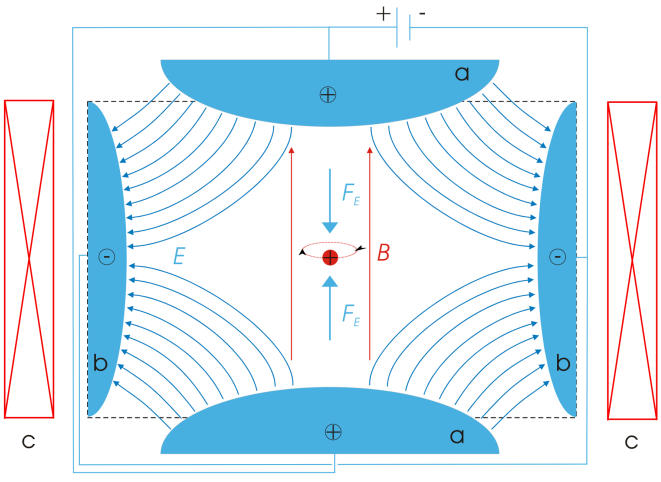

FIG. 1. The schematic of our Penning trap. The illustration is by Arian Kriesch and taken from Wikimedia Commons.

The next step to get a better understanding of how the Penning trap works is to solve the equations of motion

for a single particle inside the trap. These describe the trajectory of the particle over time. Since there is only one particle it is possible to calculate them analytically, but we will need to introduce some definitions first.

The first definition is the **Lorentz force F**. It is the force acting upon a particle with charge q from the electric field $\mathbf{E}$, the magnetic field $\mathbf{B}$ and the velocity of the particle $\mathbf{v}$. It is given by

$$\mathbf{F} = q\mathbf{E} + q\mathbf{V} \times \mathbf{B}. \tag{2}$$

Secondly, we need to define the time evolution of a particle. It is given by Newtons second law,

$$m\ddot{\mathbf{r}} = \sum_i \mathbf{F_i}, \tag{3}$$

Where m is the mass of the particle and $\ddot{\mathbf{r}}$ is the acceleration. Now we have enough information to derive the equations of motion of the single particle. For simplicity we assume that the charge $q > 0$. We start with rearranging Newtons second law given in equation 3, removing the summation sign since we only have one particle.

$$\ddot{\mathbf{r}} = \frac{1}{m}\mathbf{F} = \frac{q}{m}\left(\mathbf{E} + \mathbf{v} \times \mathbf{B}\right), \tag{4}$$

where

$$\mathbf{E} = -\nabla V = \frac{V_0}{d^2}\left(x, y, -2z\right), \tag{5}$$

$$\mathbf{v} = (v_x, v_y, v_z), \tag{6}$$

$$\mathbf{B} = (0, 0, B_0), \tag{7}$$

$$\mathbf{v} \times \mathbf{B} = \left(v_y B_0, -v_x B_0, 0\right). \tag{8}$$

Putting everything back into equation 4 we get the following:

$$\ddot{\mathbf{r}} = \omega_z^2\left(\frac{1}{2}x, \frac{1}{2}y, -z\right) + \omega_0(v_y, v_x, 0). \tag{9}$$

where we define $\omega_o \equiv \frac{qB_0}{m}$, and $\omega_z^2 \equiv \frac{2qV_0}{md^2}$. This is equivalent to the system of equations below:

$$\ddot{x} - \omega_0 \cdot \dot{y} - \frac{1}{2}\omega_z^2 \cdot x = 0, \tag{10}$$

$$\ddot{y} + \omega_0 \cdot \dot{x} - \frac{1}{2}\omega_z^2 \cdot y = 0, \tag{11}$$

$$\ddot{z} + \omega_z^2 \cdot z = 0. \tag{12}$$

These three equations describe the trajectory of a single particle. We see that the equations representing the xy-plane are coupled, while the equation governing the axial motion is independent. This introduces some difficulty solving the first two equations, but the general solution to equation 12 is easy to obtain. The general solution in the z-plane is derived in appendix [A] and gives the following result:

$$z(t) = c_1 \cos(\omega_z t) + c_2 \sin(\omega_z t). \tag{13}$$

Solving the coupled differential equations 10 and 11 is not as straight forward. In appendix [B] we introduce the complex function $f(t) = x(t) + iy(t)$, and use it to write the equations 10 and 11 as a single differential equation

$$\ddot{f} + i\omega_0 \dot{f} - \frac{1}{2}\omega_z^2 f = 0. \tag{14}$$

This allows us to calculate the general solution for f, which is

$$f(t) = A_+ e^{-i\omega_+ t} + A_- e^{-i\omega_- t}, \tag{15}$$

where

$$w_\pm = \frac{\omega_0 \pm \sqrt{w_0^2 - 2w_z^2}}{2}. \tag{16}$$

The function $f(t)$ represents the movement of the particle in the xy-plane. Where there are two forces acting on our single particle. The electric field is pushing it outwards, while the magnetic field is spinning it around. The fields are moving the particle in different directions, and in the ideal situation they create an area of equilibrium where the particle is trapped. The next step is to calculate the necessary constraints that ensures the entrapment of the particle. This means that we need to find a solution where $|f(t)| < \infty$ as $t \to \infty$.

We see from equation 16 that we need $\omega_0^2 > 2\omega_z^2$, or equivalently $\omega_0 > \sqrt{2}\omega_z$. This brings us to the following relation

$$\omega_0^2 > 2\omega_z^2 \iff \frac{q^2 B_0^2}{m^2} > \frac{4qV_0}{md^2} \iff \frac{q}{m} > \frac{4V_0}{d^2 B_0}.$$

This ratio can be used to find the optimal Penning trap parameters d, B_0 and V_0. For instance, if q/m is very small, you could make the characteristic dimension larger, the applied potential smaller, the field strength stronger or a combination of all three. Intuitively this makes sense because we want the magnetic field to 'win' over the electric field, preventing the particle from being shot out of the trap.

We have found the right parameters that ensures the success of the Penning trap depending on the mass and charge of the particles. Next, we want to get a better understanding of the movement of the particles inside the

trap. A natural first step is to find an upper and lower bound for the particles distance from the origin in the xy-plane. Using Euler's formula in appendix [C] we can use the general solution in equation 15 to find the upper and lower bounds creating our region of movement. $R_\pm$ is solved in appendix [D] and is given by

$$R_+ = |A_+ + A_-|, \quad R_- = |A_+ - A_-|. \tag{17}$$

A visualization of the possible movement of the region is given in figure 2.

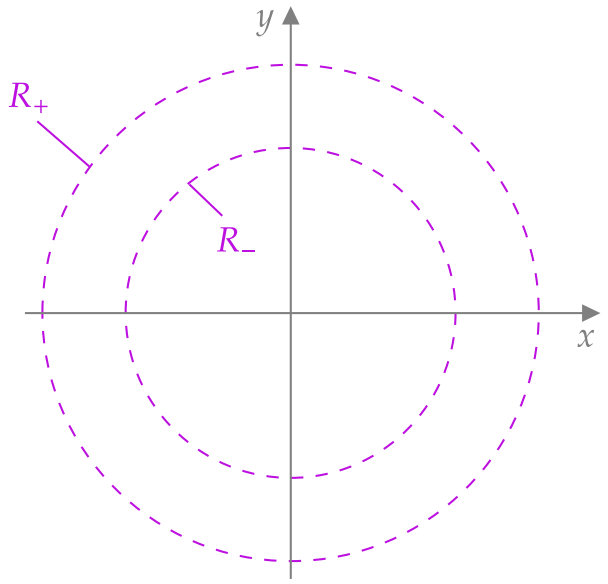

FIG. 2. This diagram shows the constraints on the movement of a particle in the xy-plane. The particle will move in the region between the outer bound $R_+ = |A_+ + A_-|$ and the inner bound $R_- = |A_+ - A_-|$.

We have enough information to begin a simulation of the Penning trap. It would, however, not be very useful without a way to validate our results. Therefore, we will find a specific analytical solution to use for comparison before we start the simulations. We find a specific solution to $f(t)$ in appendix [E], and it is given by

$$f(t) = \frac{v_0 + \omega_- x_0}{\omega_- - \omega_+} e^{-i\omega_+ t} - \frac{v_0 + \omega_+ x_0}{\omega_- - \omega_+} e^{-i\omega_- t}. \tag{18}$$

Now we impose the initial conditions along the z-axis to attain a specific solution for our initial value problem. Calculated in appendix [F] we get

$$z(t) = z_0 \cos(\omega_z t). \tag{19}$$

Now we have obtained three equations that analytically solves the motion of a single particle in a idealized Penning trap, which are the equations D1, D2 and 19, given respectively as;

$$x(t) = A_+ \cos(\omega_+ t) + A_- \cos(\omega_- t), \tag{20}$$
$$y(t) = -A_+ \sin(\omega_+ t) - A_- \sin(\omega_- t), \tag{21}$$
$$z(t) = z_0 \cos(w_z t). \tag{22}$$

The definitions of A_- and A_+ are given in the appendix by equations E7 and E8. A visualization of the motion is given in figures 3 and 4. Figure 3 shows the motion in the radial plane, while figure 4 shows the whole movement in three dimensions.

B. Numerical Methods

We have solved the equations of motion for a single particle in an idealized Penning trap, but what happens when we add more particles to the trap? When there are multiple particles in the trap, they all get coupled equations of motion. This is because each particle not only experiences the force from the electric and magnetic fields of the Penning trap, but also the Coulomb force from the other particles. For a set of n particles with charges $\{q_1, \ldots, q_n\}$ and masses $\{m_1, \ldots, m_n\}$ the set of equations becomes

$$\ddot{x}_i - \omega_{0,i}\dot{y}_i - \frac{1}{2}\omega_{z,i}^2 x_i - k_e \frac{q_i}{m_i} \sum_{j \neq i} q_j \frac{x_i - x_j}{|\mathbf{r}_i - \mathbf{r}_j|^3} = 0, \tag{23}$$

$$\ddot{y}_i - \omega_{0,i}\dot{x}_i - \frac{1}{2}\omega_{z,i}^2 y_i - k_e \frac{q_i}{m_i} \sum_{j \neq i} q_j \frac{y_i - y_j}{|\mathbf{r}_i - \mathbf{r}_j|^3} = 0, \tag{24}$$

$$\ddot{z}_i + \omega_{z,i}^2 z_i - k_e \frac{q_i}{m_i} \sum_{j \neq i} q_j \frac{z_i - z_j}{|\mathbf{r}_i - \mathbf{r}_j|^3} = 0, \tag{25}$$

This set of coupled differential equations work for an arbitrary number of particles with particle indices i and j. However, it will not be possible to solve the equations analytically as we did in the previous section. This is because the Coulomb force makes the equations 23, 24 and 25 non-linear. And as mentioned in the introduction: non-linear equations are often unsolvable analytically. Therefore we turn to numerical methods. Specifically, we will consider two famous numerical methods: The trustworthy Euler Cromer method (ECM) and the more accurate, but costly, Runge-Kutta 4 method (RK4M).

The ECM evaluates the velocity at a given point v_i and the scaled function hf_i. This gives us the oncoming velocity v_{i+1}. With the oncoming velocity, ECM takes us from an approximated point (x_i, t_i) to the next approximated point (x_{i+1}, t_{i+1}) by following the tangent line. This result is inferred in [5] and results in the approximation

$$v_{i+1} = v_i + hf(t_i, x_i), \tag{26}$$
$$x_{i+1} = x_i + hv_{i+1}, \tag{27}$$

where $f(t_i, x_i) = a_i$. This approximation is repeated for each time-step. Each time-step introduces a local error of order $\mathcal{O}(h^2)$, though for N steps the global error becomes $N\mathcal{O}(h^2) \approx \mathcal{O}(h)$. [5] This means that if the step size is halved, the error will also be halved. Although the algorithm is easy to implement and have relatively few FLOPs, we could do much better in terms of accuracy.

The RK4M is the main numerical method we will use in this project. It addresses some of the drawbacks of the ECM and is a considerably more accurate approximation to our differential equations. For each time-step the method uses several evaluations of the function f to achieve a higher accuracy. The RK4M is, as the name implies, a fourth order numerical Runge-Kutta method, which means that the error term is of order four. Hence when the time-step is halved, the error will be sixteen times smaller. This is a great improvement compared to the ECM, which would only halve the error, although it comes at the cost of a few more FLOPs. The algorithm iterates over the following approximation: [5]

$$\begin{aligned}
\mathbf{k}_0 &= \mathbf{f}(t_k, \mathbf{x}_k), \\
\mathbf{k}_1 &= \mathbf{f}(t_k + h/2, \mathbf{x}_k + h\mathbf{k}_0/2), \\
\mathbf{k}_2 &= \mathbf{f}(t_k + h/2, \mathbf{x}_k + h\mathbf{k}_1/2), \\
\mathbf{k}_3 &= \mathbf{f}(t_k + h, \mathbf{x}_k + h\mathbf{k}_2), \\
\mathbf{x}_{k+1} &= \mathbf{x}_k + \frac{h}{6}(\mathbf{k}_0 + 2\mathbf{k}_1 + 2\mathbf{k}_2 + \mathbf{k}_3). \qquad (28)
\end{aligned}$$

III. RESULTS AND DISCUSSION

Since we have an analytical solution of a particles movement in a Penning trap, it can be useful to visualize this before we do a simulation with Runge-Kutta, to observe how we expect the particles trajectory to behave.

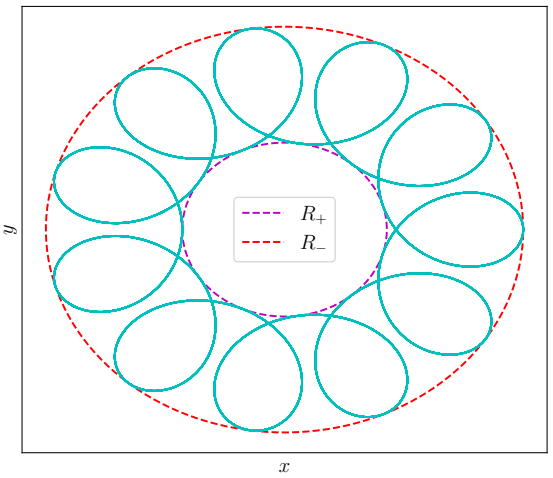

FIG. 3. The trajectory of a single particle plotted in the radial plane given by the equations 20 and 21. We have used $A_+ = 2$, $A_- = -5$, $\omega_+ = 5$ and $\omega_- = -0.5$. The particle's trajectory arises due to the electric field, which pushes the particle outwards, while the magnetic field rotates it around. You can clearly see how R_+ and R_- constrain the movement of the particle.

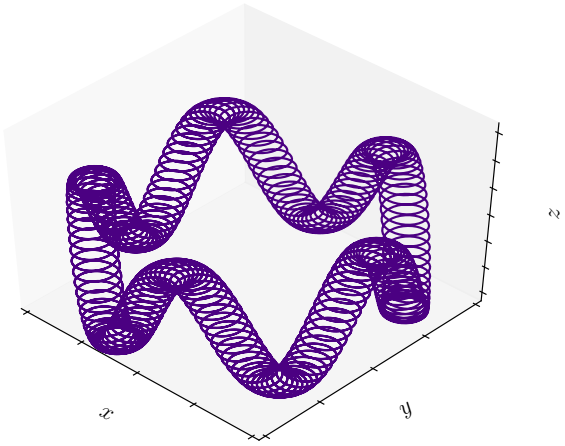

FIG. 4. The analytical solution plotted in a 3-dimensional space given by the equations 20, 21 and 22. We have used $A_+ = 10$, $A_- = -1.5$, $\omega_+ = 0.1$, $\omega_- = -20$, $z_0 = 1$ and $\omega_z = 0.5$.

The particle trajectory have two distinct motions, one in the axial-plane and one in the radial plane. The motion in the axial plane is shown in figure 3. It shows how the electric field and the magnetic field both push the particle in different directions. The result is the spinning motion from figure 3. The motion in the axial plane is more straight forward. Since the particle is stable in

the z-direction, it will follow a simple cosine movement. Figure 3 shows an example of the axial movement of a particle. Figure 4 shows both the radial and axial movement in the same plot.

The trajectories can vary strongly depending on the chosen initial conditions, but they will all follow the same basic pattern. From equations 20, 21 and 22, we can see how the initial conditions will affect the trajectory. For instance, z_0 and ω_z will change the amplitude and frequency of the axial motion. The same holds for A_+/A_- and ω_+ / ω_-; they will control the amplitude and frequency of the spinning motion around the centre, shown in figure 3. Intuitively, you can think that A_+ and A_- controls the upper and lower bounds for the particles distance to the center of the trap. Those bounds are represented as R_+ and R_-. While the amount of spinning you get in the radial plane is controlled by ω_+ and ω_-.

Now that we have set some basic expectations for how a single particle will behave inside the Penning trap, it is time to simulate it. We start off by simulating particles without particle interaction, to see if they move in a trajectory similar to the ones we found using the analytical solution. For the experiments we will use singly charged Calcium ions (Ca^+), which has an elementary charge of $2q$ and an atom mass of $40,078u$. (All code used for the simulation can be found in [6])

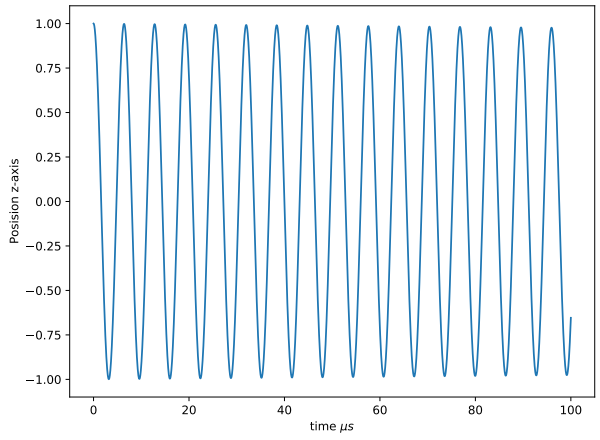

FIG. 5. Plot of z against $t \in [0, 100]$ in milliseconds. The plot represents the different heights our particle move through. We have an electric field $\mathbf{E}$ given in equation 5 and a magnetic field $\mathbf{B}$ given in equation 7 affecting the particle. The initial condition we set for z was $z_0 = 1.0$.

In figure 5 we observe that the frequency $\omega = 2\pi/T \approx 1.005$, where $T \approx 100/16 = 6.25$ and its supposed equal angular velocity $\omega_z = \sqrt{\frac{2qV_0}{md^2}} = 0.96$ match, and their values correlate. We see a symmetrical wave of values where the particle's z-position never goes over $|z| = 1$. This shows that the electric field manages to contain the particle within a certain bound in the z-direction.

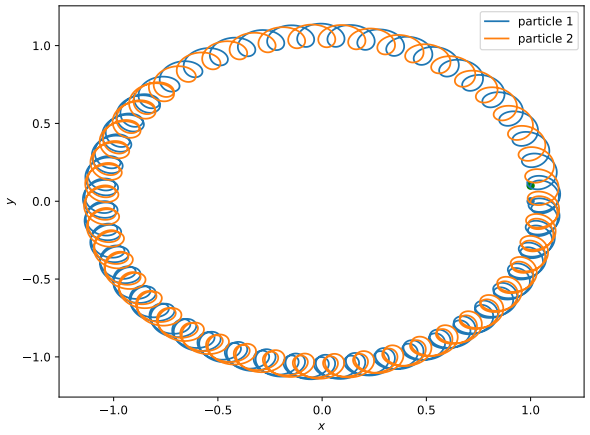

FIG. 6. Plot in the xy-plane without interactions. In this plot we made two equal particles with equal initial conditions, except for y_0, which we set $0.1\mu m$ away from each other. The initial conditions were $\boldsymbol{r}_1 = [x_0, y_0, z_0] = [1.0, 0.1, 1.0]$ and $\boldsymbol{r}_2 = [1.0, 0, 1.0]$. The same forces are in action as in figure 5.

In contrast to figure 5, we want to model the axial motion in figure 6. We observe that both particles move in a rotating motion and their trajectory is almost identical. None of the particles breaks away from the Penning trap. In figure 5 and figure 6 we observe a trajectory as expected from figure 4 and figure 3. We can therefore conclude that our numerical simulation of a Penning trap works for the interaction between the Penning trap and a particle. We then want to implement interactions between particles by also calculating the Coulomb force between the existing particles. This is shown in figure 7.

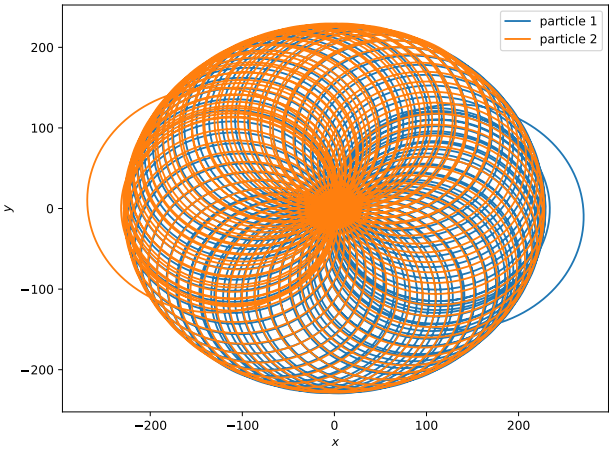

FIG. 7. Plot in the xy-plane with interactions. This plot was made with the same particles as in figure 6.

The forces between the particles in figure 7 is the

Coulomb force given in equations 23, 24 and 25. The collective forces are non-linear and are calculated numerically with the ECM and RK4M methods given in equations 26 and 28 respectively. It is clearly observed from this plot that the particles greatly affect each others trajectory. We can also observe from the figure that each particle traverses a large section of the xy-plane compared to figure 6, where both particles moved along a more identical and shorter trajectory.

Figure 7 shows us how two particles trajectories looks when we account for interaction between both of them. However, this does not capture exactly how an interaction between two particles look like. A good way to show this, is to simulate the Penning trap for just enough time to capture particles interacting, and make a figure out of this. We therefore run the simulation for step size 0.01 and total time 1 μs.

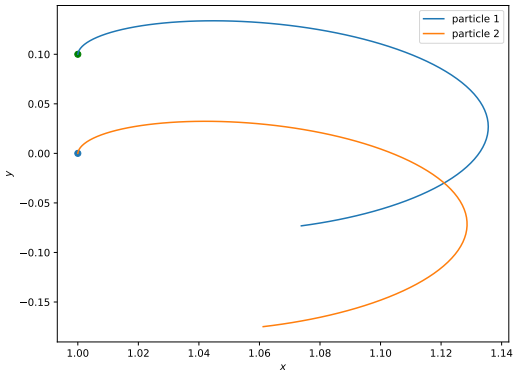

FIG. 8. Plot of two particles without interactions, over a total time of 1 μs. Here we used same particles as in figure 6 and figure 7

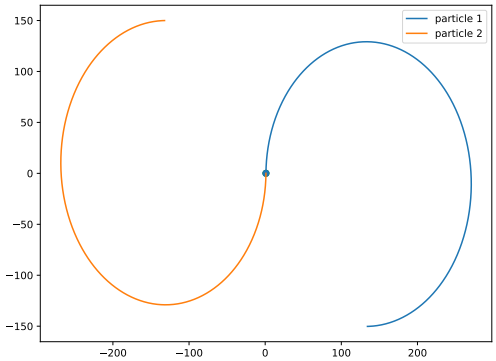

FIG. 9. Plot of two particles with interactions, over a total time of 1 μs. We used same particles as in 8.

We can clearly observe from figure 9 how particle interactions behave. The first thing we observe is that both particles push away from each other and end up in complete opposite directions. The other thing to notice is the scaling of the xy-plane compared to figure 8, which was made without particle interactions. We can see that with particle interactions, the particles end up moving approximately 1500 times further away on the y-axis, and approximately 200 times further away on the x-axis. The huge Coulomb force is a result of the particles initial positions being close to each other. This further shows the importance of including particle interaction in the Penning trap. Since the forces of the particles interacting could result in enough force to shoot a particle out of the Penning trap if we do not adjust the Electrical force of the Penning trap correspondingly.

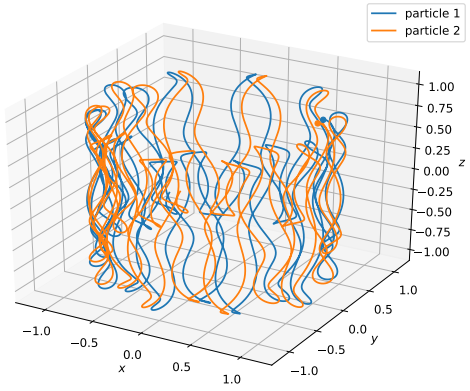

FIG. 10. 3D plot without interactions. Here we see a repeating pattern in the movement in the xyz-space. Their path is only slightly changed and a relatively small shift differentiates them as expected.

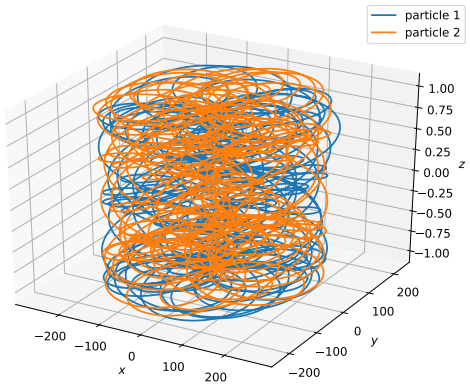

FIG. 11. 3D plot with interactions. Using the same particles as in figures 7 and 6.

Compared to figure 7, figure 11 looks more chaotic and not as repetitive as just looking at the xy-plane in figure 7.

We have now looked at the trajectory of particles with and without interactions. However, it can be useful to look at different planes, such as looking at the velocity in x, y, z direction plotted against its own dimension. This can give us a better understanding of how the velocity changes on each axis, and also at what rate and what frequency. To ensure the test to give as valuable results as possible, we position the particles close, but ensure that they have a distinct distance between each other on both xy-plane and z-axis. We set $\boldsymbol{r}_1 = [x_0, y_0, z_0] = [1.0, 0.1, 1.0]$ and $\boldsymbol{r}_2 = [1.0, 0, 2.0]$, where $\boldsymbol{r}_1$ and $\boldsymbol{r}_2$ are particles.

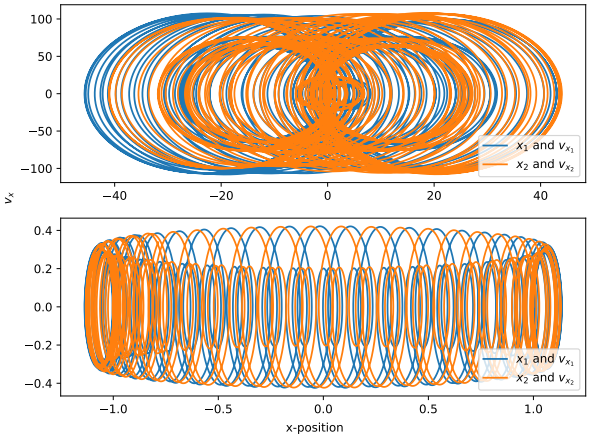

FIG. 12. Phase space plot for the (x, v_x)-plane. We calculated the velocity values by using equation 26. The upper plot is with interactions and the lower is without.

In figure 12 we observe a distinct difference between with and without interaction. The velocity is greater by as much as a factor of over 1000 when interactions occur, however, the rate in which the acceleration changes is greater when there is no interactions. We observe that in both cases their trajectory is not chaotic and predictable, the collective forces manages to contain the particles within a certain threshold. The velocity variation we observe when there is interactions corresponds well with the particle trajectories we saw on figure 7. The particles travels through a greater region when there is interaction. The interaction makes each particle pull and push on each other, making them reach towards the source of the magnetic and electric fields, however they get pushed back. This period of reaching and being pushed back is exponential and results in a high frequency. We can also notice the two paths outside the cluster when there is interactions.

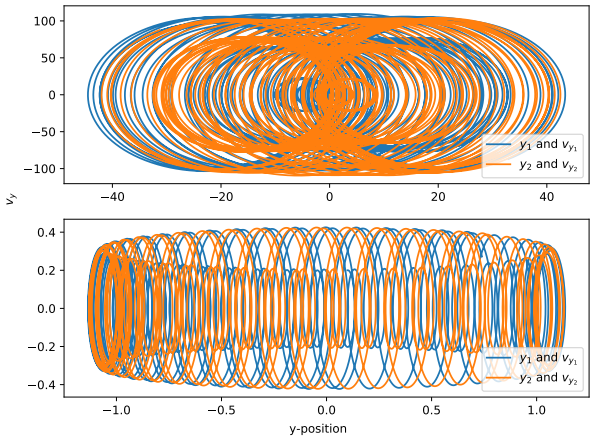

FIG. 13. Phase space plot for the (y, v_y)-plane.

We observe in figure 13 an almost identical trajectory and description of the velocity to that in figure 12.

In these plots we can see that we have vastly different plots when the particle interactions are on and when they are off. This is caused by the particles starting very close to each other, hence pushing them in opposite directions due to forces between the particles. We can see these interactions in figure 12 as the outer lines are distinctly further away than the cluster. We believe this is the result of the particles initial acceleration. At the start, the particle has a higher velocity and thus strays further away from the center. As time passes, the particles end up in a stable orbit in the Penning trap and particles stray further away from one another, and is therefore much less affected.

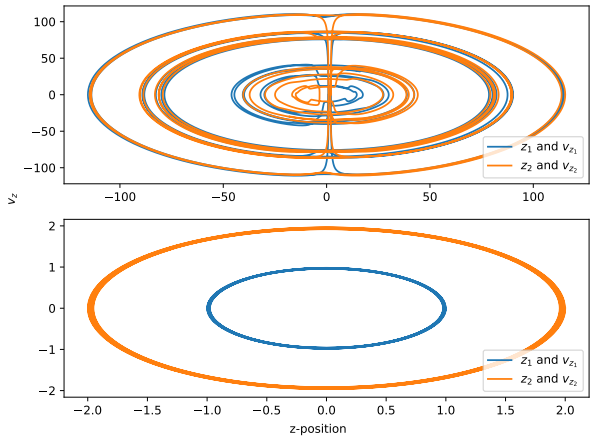

FIG. 14. Phase space plot for the (z, v_z)-plane. Upper plot is with interaction, bottom plot is without.

Compared to the phase space plots in figures 12 and 13, which represents (x, v_x)-plane and (y, v_y)-plane, in

figure 14, which represents the (z, v_z)-plane, there is a less distinct difference in the frequency of velocity change between the scenario with and without particle interaction. However, we do observe that the scale of which the particles velocity changes is almost identical for the z-axis as for the x and y-axis. This tells us that particle interaction mainly affects the scale of what velocity a particle will achieve along the z-axis, and not as much on the frequency of how often a change in velocity occurs.

We have simulated the movement of several particles with different initial conditions and trap parameters. We have also made phase space plots of the planes (x, v_x), (y, v_y) and (z, v_z). The numerical simulations have all behaved reasonably so far, but we have yet to justify our results more rigorously. Therefore we will test both our implementation of the ECM and RK4M against the analytical results shown in figure 3. This is primarily done to strengthen the validity of our implementations, but it will also reveal some important differences between the ECM and RK4M. In figure 15 you can see the relative error between the analytical equation 15 and the numerical approximations done by the ECM and RK4M respectively.

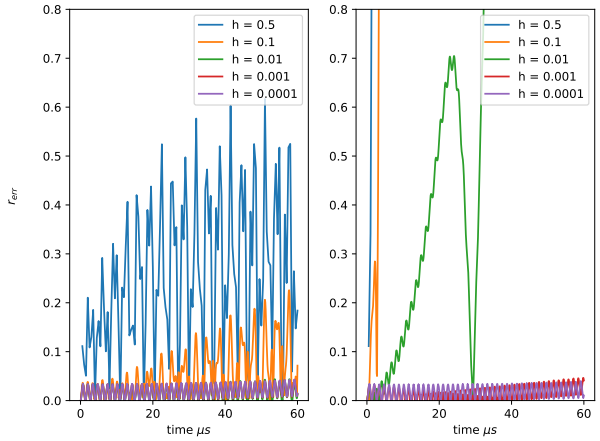

FIG. 15. Absolute error for different time step sizes. Left side was made using the RK4M and right side was made using ECM. The error is calculated using the analytical solution from equation 15.

We observe that there is, as expected, a big difference in the accuracy of the two methods. In section II B we explained how the RK4M is a fourth-order method, while ECM is a first-order method. This means that we can expect the RK4M to be stable for h-values much smaller than what ECM demands. Concerning a single particle, we see from figure 15 that the absolute error for the RK4M behaves nicely for step sizes (h) smaller than 0.01. For the larger step sizes ($h = 0.5$ and $h = 0.1$) the absolute error is significantly larger, but still relatively stable. This performance is not matched by ECM. We see that ECM is only stable for the step sizes smaller than $h = 0.001$. The other step sizes quickly diverge, hence the particle escapes the Penning trap.

The reason that the methods have large performance differences is effectively because they are different order methods. It is, however, useful to note that the problem is badly suited for the ECM. That is because it is based on linear approximations, hence it can only be exact for straight lines, which is mismatched compared to the motions we are studying. This is why the ECM tends to overshoot the real trajectory and end up spiraling out of the trap. To demonstrate more rigorously the differences in order of the two methods we will calculate the error convergence rate r_{err}.

$$r_{err} = \frac{1}{4}\sum_{k=2}^{5} \frac{\log(\Delta_{max,k}/\Delta_{max,k-1})}{\log(h_k/h_{k-1})},$$

where

$$\Delta_{max,k} = \max_i |\boldsymbol{r}_{i,exact} - \boldsymbol{r}_i|.$$

To simulate this, we need to carefully choose which values of step size we should use. Observing the graph for relative error, we can determine the range of useful step sizes to be between $0.5 - 0.1$ for the RK4M, and around 0.001 for the ECM. We therefore choose the values 0.5, 0.4, 0.3, 0.2, 0.1 for RK4M, and 0.001, 0.0012, 0.0014, 0.0016, 0.0018 for the ECM. Simulating with these step sizes, we get $r_{err} = 3.987 \approx 4$ for the RK4M, and $r_{err} = 0.9737 \approx 1$ for the ECM. These results prove what we already know to be true, which is that the RK4M is indeed a 4th-order numerical ODE solver, while the ECM is a 1st-order numerical ODE solver.

Now that we have demonstrated the accuracy of our approximations and validated the precision of our simulations, it is time to explore the physics of our virtual Penning trap. More concretely, we will study the resonance phenomena. For this purpose we will make a time-dependent perturbation of the applied potential such that

$$V_0 \to V_0(1 + f\cos(\omega_V t).$$

Here f is a constant amplitude and ω_V is the angular frequency of the time-dependent potential term. In figure 16 we have plotted the number of escaped particles for three different amplitudes f against a range of ω_V values. The simulated trap included 100 particles and a change in the parameters such that $d = 0.05cm$ and $V_0 = 0.0025V$.

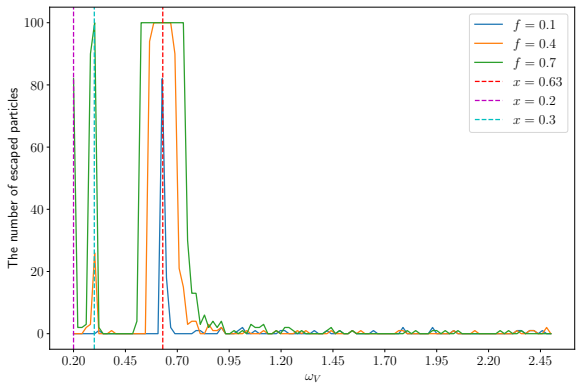

FIG. 16. Plot of the number of escaped particles from the Penning trap for different constant amplitudes f and angular frequencies ω_V. The simulated trap was filled with 100 Ca^+ particles with a randomized initial position and velocity. We have used the RK4M with a step size $h = 0.05$ over a period of 500 μs and simulated the trap for $\omega_V \in (0.2, 2.5)$ using steps of 0.02 MHz. Particle interactions are turned off.

The plot shows us that the trap undoubtedly is subject to resonance phenomena. We see three distinct peaks where many of the particles escape. In equations 20, 21 and 22 we expressed the equations of motion for a single particle as a linear combination of trigonometric functions. The movement of the particle is that of a epitrochoid. [7] Such a trajectory follows a repeated pattern. Therefore we can expect the trajectory to have a resonance frequency in the $x-$ or y-direction. The same holds for the cosine movement in the z-direction. If a frequency ω_V manages to hit close to a resonance frequency in any of the directions, we would expect the particles to gain a small momentum for each repeated pattern. This can result in particles being pushed out of the trap, where they will escape.

In addition to the three peaks, the figure 16 shows us that the number of escaped particles varies with the constant amplitude f. This is not unreasonable because a larger amplitude means that the particle will be pushed more by the electric field. And if that push corresponds to a resonating frequency then the particle will be pushed faster out of the trap. Therefore we would expect a larger constant amplitude to correspond to more particles escaping.

We can clearly see three distinct peaks, one at the very beginning ($0.2MHz$), one around 0.3 MHz and another centered around 0.63 MHz. In the x- and y directions, a particle can be expected to have frequencies depending on ω_+ and ω_-, while in the z-direction the frequency will be governed by ω_z. If we calculate the values we get $\omega_z \approx 0.31\,MHz$, which correlates nicely with the second spike in the figure. If we calculate $\omega_\pm$ for our system we get

$$\omega_+ \approx 4.8\,MHz, \quad \omega_- \approx 10^{-10}\,MHz.$$

The last and biggest spike at $0.63MHz$ is a multiple of $4.8MHz$, so we hypothesize that it is the reason we see a spike there. ω_- has a value that is much smaller than any of the ω_V-values, so it is hard to believe that it effect the particle in a major way.

In figure 17 we take a closer look at the second spike. The figure shows a scanning around the frequence 0.3 MHz which may correspond to a resonating frequency ω_z in the z-direction. We also compare the amount of particles that escape the trap when the Coulomb interactions are turned on and off.

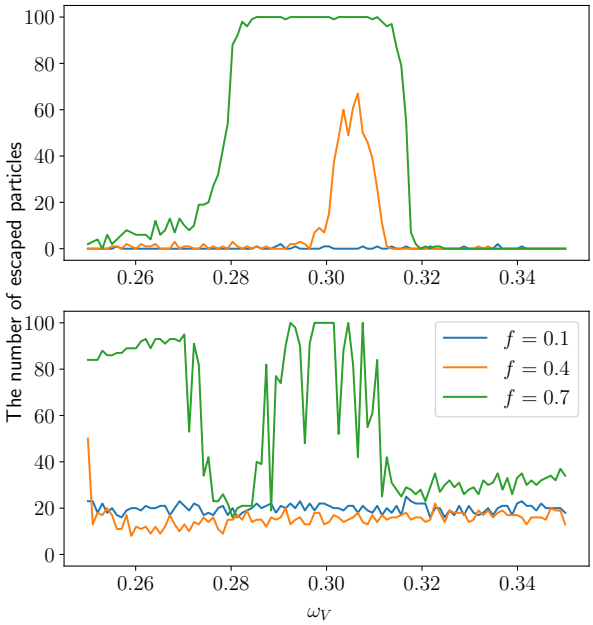

FIG. 17. Plot of the number of escaped particles against the angular frequencies ω_V for three different values of constant amplitudes f. We have zoomed in on one of the resonating frequencies $\omega_z \approx 0.3$. The top figure shows the amount of escaped particles in a Penning trap without Coulomb interactions, while the bottom has the Coulomb interactions turned on. We have used the same time-variables as in figure 16.

Interestingly, we see that the curve changes substantially when the Coulomb interactions are turned on. The Coulomb interactions manage to mitigate the effect of the resonance phenomena for $f = 0.4$. Instead of a spike where over 60 particles escape the trap, we see that it has stabilized along with $f = 0.1$ between 10 and 20 escaped particles. In the trap without Coulomb interactions, there is almost no particles escaping outside the region with resonance phenomena. When we turn on the Coulomb interactions the minimal amount of particles escaping is around 10. As we see in figure 9, two close particles will push each other away. Therefore, when particles are turned on, we can expect some particles to escape the trap independently of ω_V. Still, the plot of $f = 0.7$

makes it clear that we should still stay away from the frequencies that create resonance phenomena.

IV. CONCLUSION

We have simulated an idealised Penning trap using numerical methods. The simulation is based on two different numerical methods: ECM and RK4M. To validate our simulation, we calculated the system of differential equations for a single particle in the trap and obtained an analytical solution. In addition, the analytical result made it possible to compare the two methods and we saw that RK4M is the overall best method to simulate the trap. The error convergence rate of RK4M is four times better than FEM, which means that even though RK4M have more FLOPs it is well worth the extra computing time. We presented the simulation of a Penning trap with singly charged calcium ions Ca^+, both with and without particle interactions created by the Coulomb force. Moreover, we presented how the interaction between the particles can affect the trajectory of the movement inside the trap, and how the Ca^+ would repel each other giving them a large acceleration when the initial positions were close. Lastly, we showed that introducing a time-dependent perturbation to the applied potential introduces a resonance phenomena. These findings made it clear that when trying to create an optimal Penning trap, the trap parameters are sensitive to change. Only a 0.1 MHz change of the angular frequency or change from 0.1 to 0.7 in the amplitude can be the difference between a contained or lost particle in the Penning trap. When we turned on the particle interactions we saw that even though we stayed away from the resonating frequency 0.3 MHz, we still got particles exiting the trap.

We have found that our simulation of an ideal Penning trap is effective at trapping Ca^+ ions over a period of up to 500 μs. Depending on the mass and charge of the particles you can choose sensible trap parameters. In turn, those parameters govern the periodic motions that can cause resonance phenomena. Using sensible variables we could prevent most of the particles from escaping the trap. This demonstrated the effectiveness of the Penning trap and shows why it is used by scientists all over the world to perform studies on charged particles.

V. CODE

The code used to simulate the ideal Penning trap is available at this Github repository.

[1] R. C. Thompson, *Penning Traps*, Vol. 1 (Blackett Laboratory, Department of Physics, 2016) (accessed: 19.09.2021).
[2] M. Vogel, *Particle Confinement in Penning Traps* (Springer, Cham, 2018) (accessed: 22.09.2021).
[3] Nobel, The nobel prize in physics 1989 (2021), (accessed: 19.09.2021).
[4] Alpha, Why antihydrogen research? (2021), (accessed: 19.09.2021).
[5] M. Hjorth-Jensen, *Computational Physics*, Vol. 8 (Department of Physics, University of Oslo, 2015) pp. 245–254, (accessed: 17.09.2021).
[6] T. Tyvold, E. Kristensen, S. Gullbekk, and J. Larsen, Penning trap effects (2021), (accessed: 25.09.2021).
[7] E. W. Weisstein, Epitrochoid (2021), (accessed: 24.09.2021).

Appendix A: General z(t)

Treating

$$\ddot{z} + \omega_z^2 z = 0, \tag{A1}$$

as a second order differential equation, using the characteristic equation we derive

$$z_1 = i\sqrt{\frac{8qV_0}{md^2}} \cdot \frac{1}{2}, \quad z_2 = -i\sqrt{\frac{8qV_0}{md^2}} \cdot \frac{1}{2}, \tag{A2}$$

Then we assume a solution on the form $r(z) = e^{\alpha z}$ and substitute into equation A1

$$\frac{\partial^2 r}{\partial z^2} + \omega_z^2 r_z = e^{\alpha z}(\alpha^2 + \omega_z^2). \tag{A3}$$

Now we recognise that our substitution presents a solution on the form

$$r(z) = r(z)_1 + r(z)_2 = c_1 e^{\alpha_1 z} + c_2 e^{\alpha_2 z}, \tag{A4}$$

where α_1 and α_2 will be

$$\alpha_1 = i\sqrt{\frac{8qV_0}{md^2}} \cdot \frac{1}{2} = i\omega_z, \tag{A5}$$

$$\alpha_2 = -i\sqrt{\frac{8qV_0}{md^2}} \cdot \frac{1}{2} = -i\omega_z, \tag{A6}$$

so we get an equation which we can apply Euler's Identity on

$$r(z) = c_1 e^{i\omega_z z} + c_2 e^{-i\omega_z z}, \tag{A7}$$

$$r(z) = c_1(\cos(\omega_z z) + i\sin(\omega_z z) \tag{A8}$$

$$+ c_2(\cos(\omega_z z) - i\sin(\omega_z z). \tag{A9}$$

c_1 and c_2 are arbitrary and i is a constant, so by regrouping cos and sin we get

$$(c_1 + c_2)\cos(\omega_z z) + i(c_1 - c_2), \sin(\omega_z z) \tag{A10}$$
$$= c_1 \cos(\omega_z z) + c_2 \sin(\omega_z z), \tag{A11}$$

so our general solution is

$$r(z) = c_1 \cos(\omega_z z) + c_2 \sin(\omega_z z). \tag{A12}$$

Appendix B: Solving General f

We define $x(t) = \mathrm{Re}\, f(t)$ and $y(t) = \mathrm{Im}\, f(t)$. Then we define new functions for our coupled equations 10 and 11.

$$\mathcal{X}(x, \dot{x}, \ddot{x}) \equiv \ddot{x} - \omega_0 \cdot \dot{y} - \frac{1}{2}\omega_z^2 \cdot x = 0, \tag{B1}$$
$$\mathcal{Y}(y, \dot{y}, \ddot{y}) \equiv \ddot{y} + \omega_0 \cdot \dot{x} - \frac{1}{2}\omega_z^2 \cdot y = 0. \tag{B2}$$

Now it is obvious that since both $\mathcal{X}(x, \dot{x}, \ddot{x}) = 0$ and $\mathcal{Y}(y, \dot{y}, \ddot{y}) = 0$ for all x, y, we must also have $\mathcal{X}(x, \dot{x}, \ddot{x}) + i\mathcal{Y}(y, \dot{y}, \ddot{y}) = 0$. Lastly, since both $x(t)$ and $y(t)$ is at least twice differentiable we get $\dot{f} = \dot{x} + i\dot{y}$ and $\ddot{f} = \ddot{x} + i\ddot{y}$. Now we have enough information to rewrite $\mathcal{X}$ and $\mathcal{Y}$ as a single differential equation.

$$\begin{aligned}
\mathcal{X}(x, \dot{x}, \ddot{x}) + i\mathcal{Y}(y, \dot{y}, \ddot{y}) &= 0, \\
\ddot{x} - \omega_0 \cdot \dot{y} - \frac{1}{2}\omega_z^2 \cdot x + i\left(\ddot{y} + \omega_0 \cdot \dot{x} - \frac{1}{2}\omega_z^2 \cdot y\right) &= 0, \\
\ddot{x} + i\ddot{y} - \omega_0(\dot{y} - i\dot{x}) + \frac{1}{2}\omega_z^2(-x - iy) &= 0, \\
\ddot{f} + i\omega_0 \dot{f} - \frac{1}{2}\omega_z^2 f &= 0.
\end{aligned}$$

Appendix C: Euler's Formulae

$$e^{\pm ix} = \cos(x) \pm i \sin(x). \tag{C1}$$

Appendix D: Finding R

Using Euler's formulae from equation C1 on equation 15 we get

$$\begin{aligned}
f(t) = A_+ \cos(\omega_+ t) + A_- \cos(\omega_- t) \\
- i(A_+ \sin(\omega_+ t) + A_- \sin(\omega_- t)).
\end{aligned}$$

We recall that we can express the physical coordinates in the xy-plane as

$$x(t) = \mathrm{Re}\, f = A_+ \cos(\omega_+ t) + A_- \cos(\omega_- t), \tag{D1}$$
$$y(t) = \mathrm{Im}\, f = -A_+ \sin(\omega_+ t) - A_- \sin(\omega_- t). \tag{D2}$$

Then using the relation

$$\begin{aligned}
r(t) &= \left[x(t)^2 + y(t)^2\right]^{1/2}, \\
&= \left[A_+^2 + A_-^2 + 2A_+A_- cos(t(w_+ - w_-))\right]^{1/2}.
\end{aligned}$$

To find the actual upper and lower bounds, we look at what scenarios maximize and minimize the resulting distance. To maximize r we set $\cos(t(\omega_+ - \omega_-)) = 1$. This gives us

$$r(t) = \left[A_+^2 + A_-^2 + 2A_+A_-\right]^{1/2} = \pm A_+ \pm A_-.$$

So an upper bound on r is $A_+ + A_-$. To minimize r we set $cos(t(w_+ - w_-)) = -1$ which gives us

$$r(t) = \left[A_+^2 + A_-^2 - 2A_+A_-\right]^{1/2} = \pm A_+ \mp A_-.$$

Thus a lower bound on r is $|A_+ - A_-|$. Hence we can introduce $R_+ = A_+ + A_-$ and $R_- = |A_+ - A_-|$ such that $R_- \leq r(t) \leq R_+$.

Appendix E: Solving Specific F(t)

Using the equations for x and y given by equations D1 and D2 we calculate the derivatives

$$\dot{x}(t) = -A_+ w_+ \sin(w_+ t) - A_- w_- \sin(w_- t), \tag{E1}$$
$$\dot{y}(t) = -A_+ w_+ \cos(w_+ t) - A_- w_- \cos(w_- t). \tag{E2}$$

We then find the initial conditions

$$x(0) = A_+ \cos(0) + A_- \cos(0) = A_+ + A_- = x_0, \tag{E3}$$
$$\dot{x}(0) = -A_+ w_+ \sin(0) - A_- w_- \sin(0) = 0, \tag{E4}$$
$$y(0) = A_+ \sin(0) + A_- \sin(0) = 0, \tag{E5}$$
$$\dot{y}(0) = -A_+ w_+ \cos(0) - A_- w_- \cos(0), \tag{E6}$$
$$= -(A_+ w_+ + A_- w_-) = v_0.$$

From equation E3 we have that $A_+ = x_0 - A_-$. if we put that into equation E6 we get

$$\begin{aligned}
-(x_0\omega_+ - A_-\omega_+ + A_-\omega_-) &= v_0, \\
A_-(w_+ - w_-) &= v_0 + x_0 w_+, \\
A_- &= \frac{v_0 + x_0 w_+}{w_+ - w_-}.
\end{aligned} \tag{E7}$$

Now since $A_+ = x_0 - A_-$ we can insert the above result for A_- and get

$$A_+ = x_0 - A_- = \frac{x_0 - v_0 - x_0 w_+}{w_+ - w_-},$$
$$A_+ = \frac{x_0(1-\omega_+) - v_0}{w_+ - w_-}. \tag{E8}$$

$$f(t) = A_+ e^{-i\omega_+ t} + A_- e^{-i\omega_- t}, \tag{E9}$$
$$= \frac{x_0(1-\omega_+) - v_0}{w_+ - w_-} e^{-i\omega_+ t} - \frac{v_0 + x_0 w_+}{w_+ - w_-} e^{-i\omega_- t}. \tag{E10}$$

Appendix F: Specific z(t)

Solving equation 13 with initial conditions

$$z(0) = z_0, \quad \dot{z}(0) = 0, \tag{F1}$$

gives the specific solution

$$\dot{z}(0) = 0 = -\omega_z c_1 \sin(\omega_z \cdot 0) + \omega_z c_2 \cos(\omega_z \cdot 0), \tag{F2}$$
$$c_2 = 0, \tag{F3}$$
$$z(0) = c_1 \cos(\omega_z \cdot 0) = z_0, \tag{F4}$$
$$c_1 = z_0, \tag{F5}$$
$$\rightarrow z(t) = z_0 \cos(\omega_z t). \tag{F6}$$